JOURNAL OF APPLIED PHYSICS 101, 1 (2007)

Fabrication of polymer photonic crystal superprism structures using polydimethylsiloxane soft molds

Li Wang, Wei Jiang, Xiaonan Chen, Lanlan Gu, Jiaqi Chen, and Ray T. Chen[a]
Microelectronics Research Center, University of Texas at Austin, Austin, Texas 78758 and Department of Electrical and Computer Engineering, University of Texas at Austin, Austin, Texas 78758

(Received 15 November 2006; accepted 16 March 2007)

We presented a soft lithography technique of fabricating polymer photonic crystal superprism structures using elastomeric polydimethylsiloxane templates. Dense two-dimensional photonic crystal superprism structures with feature sizes of 150–500 nm and aspect ratios of up to 1.25 were replicated. Large field size and easy fabrication are two major advantages when compared with other imprint technology. Atomic force microscopy images showed that the molded structures had high fidelity to the masters. Less than 3% reduction of the depth in the molded structures was achieved with respect to the master. The increase of the surface roughness from the master to the molded structures is minimal. The issue of pattern collapse during pattern transfer of submicron structures was analyzed against the pattern dimensions and aspect ratios; and the experimental results were found in agreement with a prior theory. We also experimentally demonstrated the superprism effect in two-dimensional photonic crystal structure at near-infrared wavelength. The propagation beam changed 39° in the photonic crystal with respect to the input wavelength varying from 1546 to 1572 nm. Such an effective, low cost, and high throughput soft lithography technique could find wide use in making photonic crystal based nanostructures. © 2007 *American Institute of Physics*. [DOI: 10.1063/1.2732545]

AQ: #1

INTRODUCTION

Nanophotonics shows the promise to have a revolutionary impact on the landscape of photonics technology. Photonic crystal based nanostructures are anticipated to play a significant role in next generation photonic devices. Photonic crystals are artificial dielectric periodic structures. They can form functional photonic devices with significantly reduced sizes and prominent characteristics, such as high wavelength and angular sensitivity[1] and significant group velocity dispersion.[2,3] Recently, devices based on two-dimensional (2D) photonic crystal slabs have stirred up widespread interest as such 2D planar photonic structures are compatible with conventional microelectronic and photonic devices. Myriads of optical components such as waveguides, resonators, demultiplexers, and modulators have been designed and fabricated based on 2D photonic crystal geometry.[1–6]

Polymers, a class of materials that can be integrated with virtually all other substrates, have been considered as a promising material candidate for photonic crystals. Polymer photonic crystal slabs usually do not exhibit complete photonic band gaps because of low dielectric constants of polymers. However, certain optical devices such as superprism based demultiplexers do not require the photonic crystals to have a band gap.[7]

To fabricate polymeric photonic crystals, many efforts have been focused on conventional processing techniques such as electron-beam (e-beam) nanolithography and reactive ion etching (RIE), which are relatively complicated, costly, and time consuming. Imprint lithography is one of the promising methods for making microstructures and nanostructures owing to low cost and high throughput. Most prominent among these methods are hot embossing, step and flash imprint lithography (SFIL), and soft lithography.[8–17] Hot embossing lithography employs a silicon or nickel template to imprint the resist above its glass transition temperature with large pressure applied. The heating cycle extends the process time and pattern distortion can occur due to high temperature and large pressure. The imprint area is limited by the waviness of the substrate. SFIL can be used to imprint high resolution patterns over a large area by step and repeat. However, imprinting on a 100 mm wafer size can be realized using polydimethylsiloxane (PDMS) template in one single step.[18] Soft lithography utilizes elastomeric PDMS with relief patterns to replicate micro- and nanostructures.[9] A PDMS template is generally prepared by casting prepolymer against a master patterned by conventional lithography techniques. One advantage of soft lithography that utilizes PDMS rather than ridged template is that it can conform to a substrate over large areas without external force. A second advantage of PDMS is that it is easily removed from the master and molded structures. For hot embossing and SFIL, it is necessary to coat an antisticking layer on the template to completely release it from the imprinted polymer. Even though the template surface is treated with a low surface energy surfactant, the imprinted polymer tends to adhere to the template and cause defects when imprinting dense or high aspect ratio patterns.[19]

The line and hole structures at nanoscale with aspect ratio considerably smaller than 1 were demonstrated using soft lithography in recent years.[10,14] However, it becomes challenging to replicate structures with aspect ratios larger than 1 and feature sizes smaller than 500 nm in part because

---

[a] Electronic mail: raychen@uts.cc.utexas.edu

0021-8979/2007/101(9)/1/0/$23.00

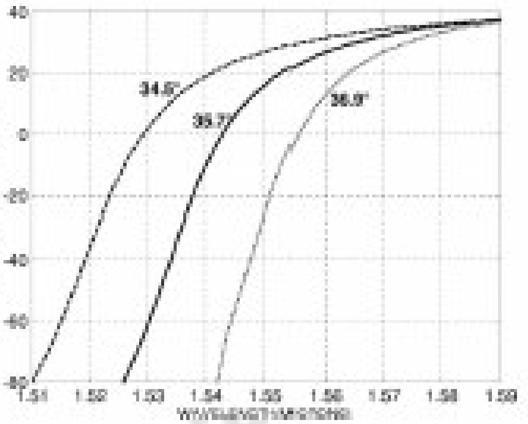

FIG. 2. (Color online) Propagation angle as a function of the normalized frequency for different incident angles.

of the low modulus of PDMS. These features are desired in many soft lithography applications such as fabricating photonic crystals. When the feature size shrinks to submicro- or nanoscale, the aspect ratio (depth/width) and pattern density (width/spacing) play an important role in the PDMS deformation. For high aspect ratio structures, lateral collapse can easily occur owing to capillary and other forces during the pattern transfer of submicron structures.[20] In this work, we employed soft lithography to fabricate fine structures with aspect ratios larger than 1 and feature sizes in the range of 100–500 nm. We also investigated the deformation of PDMS in making dense photonic crystal patterns.

SIMULATION

Before the fabrication of the 2D polymer photonic crystal, the photonic crystal superprism structure with a triangle array of air holes was designed and calculated. The refractive index of background polymer is 1.475 at 1550 nm. To optimize the design of superprism for low index contrast photonic crystals, the complete band structure and the dispersion surface were calculated and analyzed by the plane wave expansion.[21] Figure 1(a) shows the calculated band structure of a triangle lattice with a polymer refractive index of 1.475. The hole radius is $r=0.25a$, where a is the lattice constant. The inset shows the first Brillouin zone and its symmetry points. There is no complete photonic band gap for transverse electric (TE) mode (electric field parallel to the plane) and transverse magnetic (TM) mode (magnetic field parallel to the plane) due to low refractive index contrast.

The dispersion surface is determined by the band structure in various directions. For a given incident wave vector, the propagation direction can be obtained through the momentum conservation rule and group velocity $v_g = \nabla_k \omega(\mathrm{k})$ which is normal to the dispersion surface.[1] The dispersion surface of the first band (TE mode) is shown in Fig. 1(b). At low normalized frequency ($\omega a / 2\pi c < 0.4$), the band structure is isotropic and the dispersion surface is circlelike with a radius given by the magnitude of wave vector. For the normalized frequencies in the range of 0.4–0.45, the band structure is strongly anisotropic and the dispersion surface is distorted from circle. The propagation direction is sensitive to the wavelength of incident light and incident angle at the sharp corner region of the dispersion surface. Figure 2 shows the propagation angle in the photonic crystal as a function of the wavelength for the different incident angles. The photonic crystal structure is an array of air holes in the polymer with 325 nm in diameter (lattice constant of 650 nm). For the incident angle of 36.9°, the propagation angle changes from −51° to 28° when the wavelength of the incident light is varied from 1546 to 1572 nm.

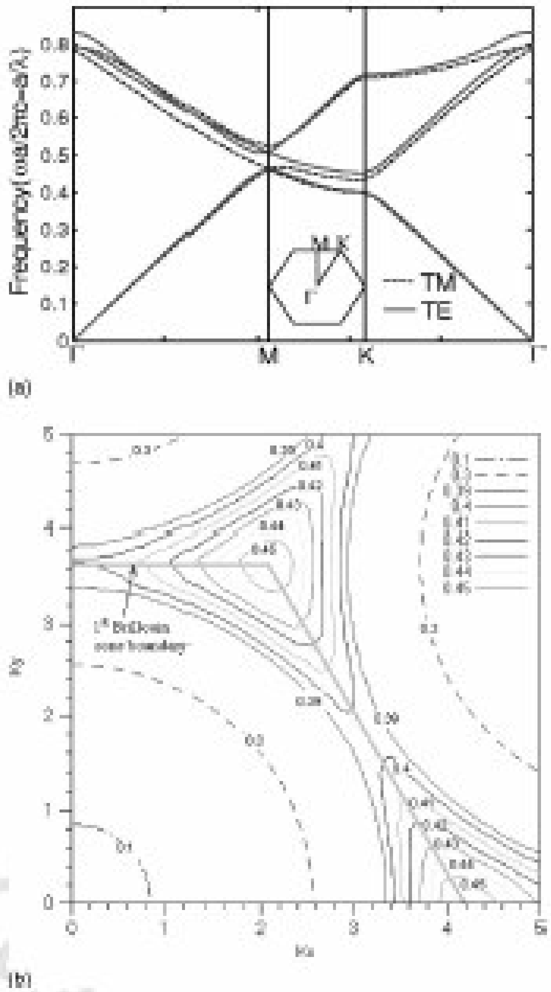

FIG. 1. (Color online) (a) Photonic band structure of a triangle array of air holes on the polymer with a polymer refractive index of 1.475. (b) Contour curve of dispersion surface of the first band (TE mode).

The superprism is a large area defect-free structure. The simulation results show that the feature size of the superprism is in the range of hundreds of nanometers. It can be fabricated on a large area in one step using soft lithography.

FABRICATION

Soft lithography is used to fabricate the photonic crystal structures. There are three steps in the soft lithography procedure: (1) master fabrication, (2) PDMS template formation, and (3) pattern transfer.

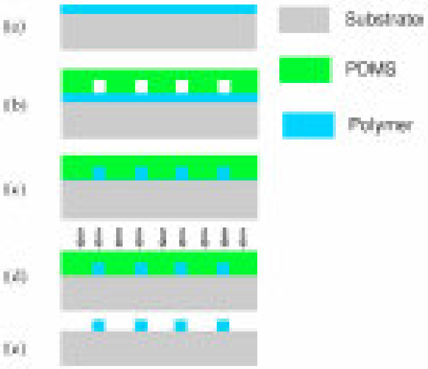

FIG. 3. (Color online) Schematic diagram of the soft lithography process: (a) polymer was dispensed on the substrate; (b) PDMS template was placed on the substrate; (c) filling of the space by capillary; (d) the polymer was cured by UV light; and (e) PDMS template was released.

Master fabrication

We fabricated the master structures composed of triangular arrays of identical holes using a JEOL JBX6000 electron-beam lithography (EBL) system. The diameter of the holes ranges from 100 to 500 nm, and the period from 200 to 1000 nm. First, a layer of e-beam resist (ER) ZEP520A was coated on a silicon substrate. The patterns were defined by EBL and the exposed ER was developed in the ZED-N50 solution. After developing, it was postbaked on a 100 °C hotplate for 10 min. A 2D triangular array of holes was thus fabricated on the ER.

PDMS template formation

The PDMS material (Sylgard 184, Dow Corning) is composed of two parts, the base and the curing agent. They were mixed at a ratio of 10:1 in weight and were degassed in vacuum to eliminate air bubbles. Then we poured PDMS prepolymer onto the master and cured it on a hot plate at 60 °C for 12 h. The Young's modulus of PDMS is 2 MPa.[22] Because the cured PDMS did not adhere to the resist patterns, it could be easily peeled off from the master. The 2D photonic crystal structures were transferred from the master to the PDMS template. The holes on the master yield the posts on the PDMS template.

Pattern transfer

The procedures of soft lithography are shown in Fig. 3. A small amount of UV curable acrylate polymer (WIR30-470, ChemOptics, Korea) is dispensed evenly on the substrate. The PDMS template is then placed in contact with the substrate without any external force. The capillary force drives the polymer to fill the void spaces of the template, leading to pattern formation. The low viscosity of polymer WIR30-470 (0.2 Pa s) allows the rapid filling of the recessed features of PDMS on the order of microseconds, which were estimated based on the surface tension and viscosity of the polymer.[23,24] The PDMS template and substrate remain in contact until the polymer fills the void spaces of the template. Then the prepolymer is cured by exposure to UV radiation through the transparent PDMS template. The transmission of a 3-mm-thick PDMS block was measured to be 91% at 365 nm using a Cary 5000 UV-visible-near infrared (NIR) spectrometer. The PDMS template is subsequently peeled off, leaving a triangular lattice of holes on the WIR30-470 polymer. By using the above procedures, the transfer of photonic crystal patterns is realized. The samples are postbaked to further remove solvents in the polymer.

FABRICATION RESULTS AND DISCUSSION

By the above procedures, the 2D photonic crystal structures were fabricated by soft lithography. The profile of the molded structures was examined by scanning electron microscopy (SEM) and atomic force microscopy (AFM). Since AFM can provide subnanometer vertical resolution, it is suitable for the depth and surface roughness measurements of micro- and nanostructures. Measurements were carried out with a Digital Instruments AFM Dimension 3100 and the tapping mode was utilized to avoid surface modification during the measurement. The silicon probe (Veeco) with a tip height of 17.5 μm and cone half angles of 15° side, 15° front, and 15° back was used in the measurements. 2D triangle photonic crystal structures with air holes of 300 nm in diameter were shown in Fig. 4(a). The depth of air holes was 375 nm on average measured by AFM shown in Fig. 4(b). The images clearly demonstrated that an array of air holes of 300 nm diameter with an aspect ratio of 1.25 were replicated using soft lithography. For reference, we also fabricated arrays of narrow lines, which can be regarded as one-dimensional (1D) photonic crystals or gratings, by the same technique. The SEM of the grating structures were shown in Fig. 5. In Fig. 5(a) the line width, period, and depth are 150, 650, and 122 nm, respectively. In Fig. 5(b) the line width is 200 nm, the period is 400 nm and the depth is 122 nm. It shows that the resolution of molded structures was down to 150 nm with an aspect ratio of 0.81 using the soft lithography technique. During the pattern transfer from a master to a PDMS template, some problems can arise, such as air bubbles being trapped in the holes on the master due to the submicron structures with high pattern density. In previous work, a reduction of more than 10% in depth from the master to PDMS template was reported.[25] Figure 6 shows the AFM images and section analysis of the master [in Fig. 6(a)], PDMS template [in Fig. 6(b)], and molded structures [in Fig. 6(c)]. The depths of holes on each sample were analyzed along three different crystallographic directions using a software (NANOSCOPE III VERSION 6.12R1, Nanoscope, Multimode, DI-Veeco Instruments, Inc.). The three groups of line profile in the middle column of Fig. 6 show the uniform depths and periods of the hole/posts patterns along different crystallographic directions. On average, the depths of master, PDMS template, and molded structures are 387, 379, and 375 nm, respectively. We also measured the film thickness of the master structure by using a NANO SPEC microscope. The thickness of e-beam resist spin coated by 3200 rpm for 1 min on the silicon substrate is 387 nm on average. The film thickness measurements agree well with AFM measurements. There is a 3% reduction of depth in the molded structures with respect to the master. There were two steps in-

AQ: #2

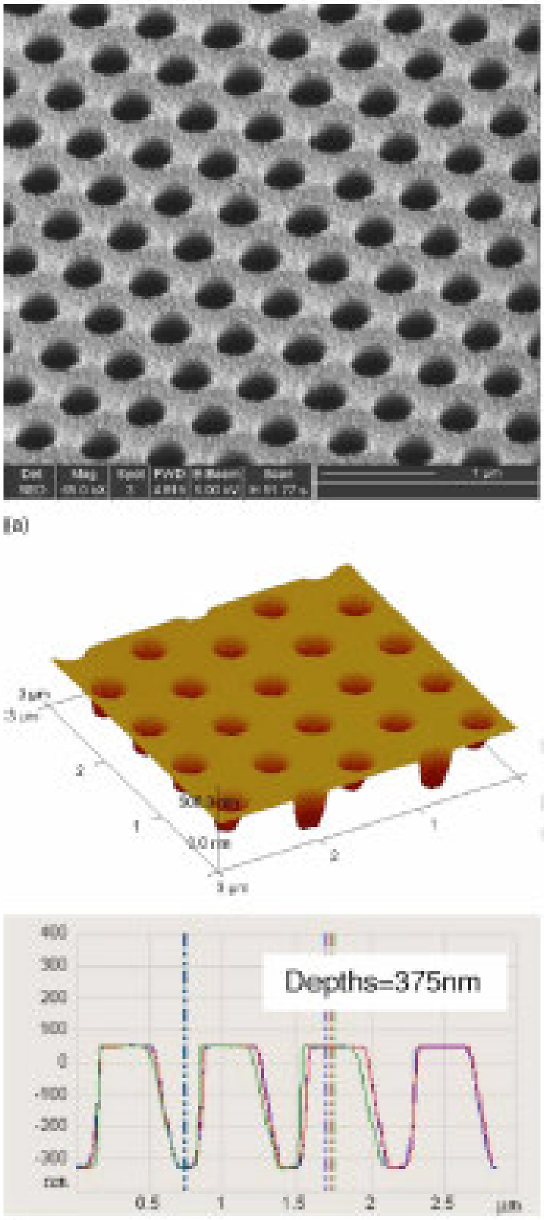

(a)

(b)

FIG. 4. (Color online) (a) SEM micrographs of the 2D molded structures with 300 nm in diameter (lattice constant of 600 nm). (b) AFM images of the 2D molded structure with 375 nm in depth.

volved in the pattern transfer. The depth reductions were 2% from master to PDMS template and 1% from the PDMS template to the molded polymer structures. The reduction is, we believe, primarily attributed to the fact that air is easily trapped in the holes on the master during fabricating the PDMS template. We solved this problem by tilting the master by 5°–10° with respect to the horizon. Then the PDMS prepolymer was poured on the high level side and it flowed slowly by gravity to the low level side. The experimental results show that the PDMS prepolymer (0.31 Pa s) can better fill in the nanostructures through the current procedure.

Light scattering due to surface roughness is an important source for optical loss. Sugimoto *et al.* measured the top surface roughness of a waveguide in a GaAs membrane photonic crystal on the order of 1 nm, which gives satisfactorily low optical loss.[26] We also analyzed the surface roughness of the molded structures and masters using AFM. Regarding the surface roughness, only a slight increase in the root mean square (rms) roughness ($\sim$1.2 nm) over 1 μm^2 area was observed on the molded structures with respect to the master ($\sim$1.0 nm). We used the same PDMS template to replicate a 2D triangular photonic crystal lattice for three times and the surface roughness remained at the same level.

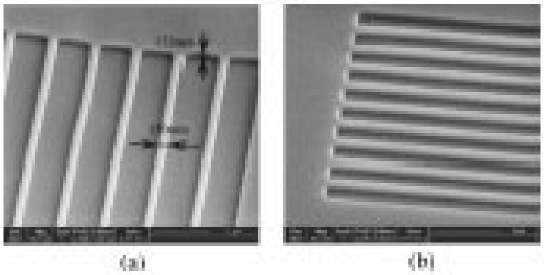
(a) (b)

FIG. 5. (Color online) SEM micrographs of the 1D molded structures.

The pattern collapse is a serious problem in submicron structures with high aspect ratios and/or high pattern density, and it is one of the factors which limit the structure dimensions. There are multiple forms of pattern collapse or defects,[20] but the lateral collapse was found to be the dominant form in our fabricated structures according to our observation. When the high aspect ratio structures are molded at high pattern density, the lateral collapse of neighboring posts occurs during the pattern transfer when the surface tension is large enough to make the neighboring posts contact. Once they contact each other, they adhere together permanently.[27] For the high pattern density or high aspect ratio, the posts become more susceptible to the surface tension. If any external force makes the posts bend and they are not vertical to the substrate, the posts are easily in contact with the neighboring posts on the top because of the small spacing between the posts.[28] The pattern density and aspect ratio of patterns therefore play an important role in the lateral collapse of PDMS templates. The condition for lateral collapse of post structures was established by Glassmaker *et al.* in 2004.[21] To be specific, the critical aspect ratio at which the collapse occurs in PDMS is given by

$$\left(\frac{h}{2a}\right)_c = \frac{1}{2}\left[\frac{27\pi^4 w^6}{32(1-\nu^2)a^2}\left(\frac{E}{\gamma_s}\right)^4\right]^{1/12}$$

$$= \frac{1}{2}\left[\frac{27\pi^4 a^4}{32(1-\nu^2)}\left(\frac{w}{a}\right)^6\left(\frac{E}{\gamma_s}\right)^4\right]^{1/12},$$

where E is the Young's modulus, a is the radius of post, $2w$ is the spacing between the posts, ν is the Poisson's ratio of PDMS ($\nu = 0.5$), and γ_s is the surface energy. The above equation describes the high density pattern having a small critical aspect ratio. For a given pattern density, the critical aspect ratio of posts becomes small as the radius decreases. The model also predicts that the stiff material (high Young's modulus) will increase the stability of posts.

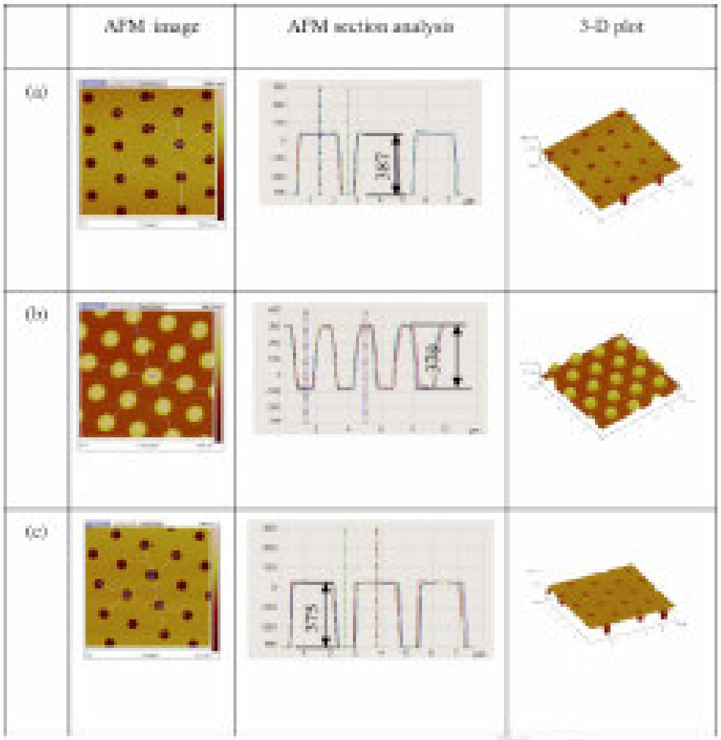

FIG. 6. (Color online) AFM images of the master, PDMS, and molded structures.

From the above equation, we can obtain the critical height (the highest height at which the patterns do not collapse),

$$h_c = \left[\frac{27\pi^4}{32(1-\nu^2)}\left(\frac{w}{a}\right)^6\left(\frac{E}{\gamma_s}\right)^4\right]^{1/12} a^{4/3}.$$

For a given pattern density $w/a = 1$, we plot the above equation in Fig. 7. The surface energy of PDMS is $55\ \mathrm{mJ/cm^2}$ measured by Chaudhury *et al.* using the JKR technique[29] and the Young's modulus of PDMS is 2 MPa.[21] The area above the line corresponds to the parameter ranges for the stable patterns and the area below the line the collapsed patterns. The 2D triangular photonic crystal lattices with different dimensions and different critical heights obtained in our experiments are also marked in Fig. 7. The dots represent those molded structures without defects; whereas the crosses represent those collapsed structures. The experimental data are in agreement with the values calculated by the above model. The critical height of 200 nm diameter holes is 122 nm. When the dimension of holes increases to 300 nm diameter, the critical height becomes 375 nm. The aspect ratio of these holes is 1.25. The critical height of 400 nm diameter holes is 490 nm. The above depths are measured by AFM.

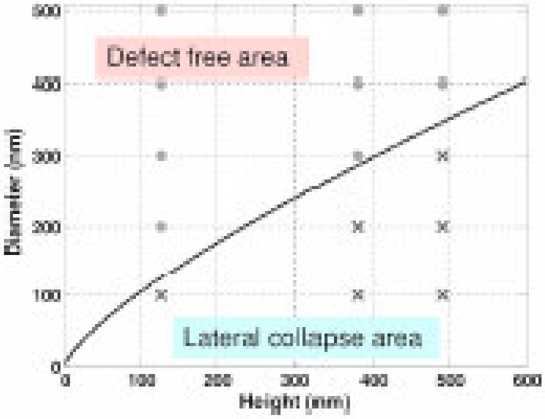

FIG. 7. (Color online) Analysis of the pattern collapse issue. The green dots represent replicated structures, whereas red crosses represent collapsed structures. The curve separating the defect-free and collapsed structures is calculated according to Ref. 28.

To avoid the collapse of PDMS templates, we can increase the Young's modulus of PDMS or use a low surface energy polymer. The Young's modulus of PDMS depends on curing time and mix ratio (base versus curing agent).[30] With curing time increasing or mix ratio decreasing, the Young's modulus will increase.

EXPERIMENTAL RESULTS

Optical measurement of the 2D photonic crystal structure with 325 nm diameter and 650 nm period was conducted using a Newport Automatic Alignment station where alignment accuracy down to 100 nm can be precisely controlled. A lensed optical fiber was used to couple a Santec tunable laser light into a fabricated sample. The input lensed fiber is aligned for the TE mode with the electric field vector primarily in plane. The TE polarized light is used for all the measurements presented here. An infrared camera was used to image the light path in photonic crystal superprism from the top surface of the sample. As the wavelength is tuned from 1546 to 1572 nm, the corresponding beam inside the 2D photonic crystal continuously changed propagating direc-

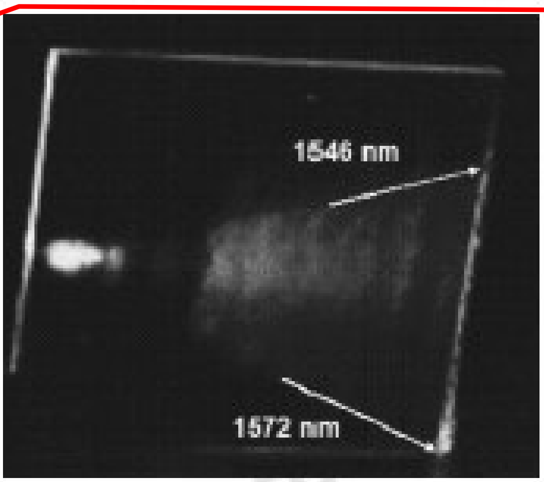

FIG. 8. (Color online) Microscope images for beam steering by wavelength: (1) beam angle at 1546 nm and (2) beam angle at 1572 nm.

tion from −19° to 20°. The beam propagation angles were shown in Fig. 8 for the beam wavelength tuning from 1546 and 1572 nm. The beam propagation direction was changed from negative to positive refraction angles with increasing wavelength. This is consistent with the numerical simulation results. The physical mechanism behind this effect can be explained with the dispersion surface. It means the shape of the dispersion surface experiences a large change with the wavelength increasing from 1546 to 1572 nm.

There is still some deviation between the experimental data and numerical simulation results. This can be caused by the imperfection of the fabricated samples. The incident light was offset from designed angle 36.9° to smaller incident angle. From the simulation results, the light propagation angle in the photonic crystal changes when the incident angle is 36.5° instead of 36.9°, while the simulation results show the propagation angle in photonic crystals changes from −26° to 27°. Reasonable agreement is obtained between the simulation results and experimental data. AQ: #4

CONCLUSION

We have fabricated the 2D photonic crystal superprism structures by soft lithography and demonstrated the superprism effect in 2D photonic crystal structure at near-infrared wavelength. The beam propagation angle changed 39° when the input wavelength was varied from 1546 to 1572 nm. An aspect ratio of 1.25 is achieved for a photonic crystal with 300 nm air holes. The depth of the master and that of molded patterns have only 3% difference. The soft lithography with PDMS templates represents a simple, low cost, and reliable approach for fabrication of fine features as small as 150 nm in linewidth without distortions or defects over a large patterned area.

ACKNOWLEDGMENTS

This work is supported in part by AFRL. The authors acknowledge the generous support from the State of Texas and Sematech through the AMRC program. The fabrication and characterization facilities at UT MRC are partially supported by NSF through the NNIN program. We thank Welch Foundation and SPRING for supporting part of the characterization facility through the Center for Nano- and Molecular Science and Technology.

[1] H. Kosaka, T. Kawashima, A. Tomita, M. Notomi, T. Tamamura, T. Sato, and S. Kawakami, Phys. Rev. B 58, R10096 (1998).
[2] A. Imhof, W. L. Vos, R. Sprik, and A. Lagendijk, Phys. Rev. Lett. 83, 2942 (1999).
[3] M. Notomi, K. Yamada, A. Shinya, J. Takahashi, C. Takahashi, and I. Yokohama, Phys. Rev. Lett. 87, 253902 (2001).
[4] W. Jiang and R. T. Chen, Phys. Rev. Lett. 91, 213901 (2003).
[5] W. Jiang, R. T. Chen, and X. Lu, Phys. Rev. B 71, 245115 (2005).
[6] Y. Jiang, W. Jiang, L. Gu, X. Chen, and R. T. Chen, Appl. Phys. Lett. 87, 221105 (2005).
[7] B. Li and R. Chen, LEOS2001, Proceedings of the 14th Annual Meeting of the IEEE, 2001 (unpublished), p. 149. AQ: #5
[8] C. R. K. Marrian and D. M. Tennant, J. Vac. Sci. Technol. A 21, S207 (2003).
[9] Y. Xia and G. M. Whitesides, Angew. Chem., Int. Ed. 37, 550 (1998).
[10] D. Pisignano et al., Nanotechnology 15, 766 (2004).
[11] S. C. Johnson et al., Proc. SPIE 5037, 197 (2003).
[12] S. Y. Chou, P. R. Krauss, W. Zhang, L. Guo, and L. Zhuang, J. Vac. Sci. Technol. B 15, 2897 (1997).
[13] L. Wang, X. Wang, W. Jiang, J. Choi, and R. T. Chen, Appl. Phys. Lett. 87, 141110 (2005).
[14] M. Bender, V. Plachetka, J. Ran, A. Fuchs, B. Vratzov, H. Kurz, T. Glinsner, and F. Lindner, J. Vac. Sci. Technol. B 22, 3229 (2004).
[15] W. Kim, K. B. Yoon, and B. Bae, J. Mater. Chem. 15, 4535 (2005).
[16] M. Belotti, J. Torres, E. Roy, A. Pépin, D. Gerace, L. C. Andreani, M. GGalli, and Y. Chen, Microelectron. Eng. 83, 1773 (2006).
[17] M. Belotti, J. Torres, E. Roy, A. Pépin, Y. Chen, D. Gerace, L. C. Andreani, and M. GGalli, J. Appl. Phys. 99, 024309 (2006).
[18] V. Plachetka, M. Bender, A. Fuchs, B. Vratzov, T. Glinsner, F. Lindner, and H. Kurz, Microelectron. Eng. 73–74, 167 (2004).
[19] L. J. Guo, J. Phys. D 37, R123 (2004).
[20] C. Y. Hui, A. Jagota, Y. Y. Lin, and E. J. Kramer, Langmuir 18, 1394 (2002).
[21] K. Sakoda, *Optical Properties of Photonic Crystals* (Springer, New York, 2004).
[22] O. D. Roure, A. Saez, A. Buguin, R. H. Austin, P. Chavrier, P. Silberzan, and B. Ladoux, Proc. Natl. Acad. Sci. U.S.A. 102, 2390 (2005).
[23] B. V. Zhmud, F. Tiberg, and K. Hallstensson, J. Colloid Interface Sci. 228, 263 (2000).
[24] T. Lee, O. Mitrofanov, and J. W. P. Hsu, Adv. Mater. (Weinheim, Ger.) 15, 1683 (2005).
[25] W. Chuang, C. Ho, and W. Wang, Opt. Express 13, 6685 (2005).
[26] Y. Sugimoto, Y. Tanaka, N. Ikeda, Y. Nakamura, and K. Asakawa, Opt. Express 12, 1090 (2004).
[27] K. G. Sharp, G. S. Blackman, N. J. Glassmaker, A. Jagota, and C. Hui, Langmuir 20, 6430 (2004).
[28] N. J. Glassmaker, A. Jagota, C. Y. Hui, and J. Kim, J. R. Soc. London Interface 1, ■ (2004).
[29] M. K. Chaudhury, T. Weaver, C. Y. Hui, and E. J. Kramer, J. Appl. Phys. 80, 30 (1996). AQ: #6
[30] D. T. Eddington, W. C. Crone, and D. J. Beebe, Proceedings of the Seventh International Conference on Miniaturized Chemical and Biochemical Analysis Systems, 2003 (unpublished).